Environ Earth Sci (2017)76:543
DOI 10.1007/s12665-017-6880-6

ORIGINAL ARTICLE

Assessing the impacts of climate and land use change on streamflow, water quality and suspended sediment in the Kor River Basin, Southwest of Iran

Amir Asadi Vaighan[1] · Nasser Talebbeydokhti[1] · Alireza Massah Bavani[2]

Received: 16 September 2016 / Accepted: 31 July 2017

Abstract This research addressed the separate and combined impacts of climate and land use change on streamflow, suspended sediment and water quality in the Kor River Basin, Southwest of Iran, using (BASINS–WinHSPF) model. The model was calibrated and validated for hydrology, sediment and water quality for the period 2003–2012. The model was run under two climate changes, two land use changes and four combined change scenarios for near-future period (2020–2049). The results revealed that projected climate change impacts include an increase in streamflow (maximum increases of 52% under RCP 2.6 in December and 170% under RCP 8.5). Projected sediment concentrations under climate change scenarios showed a monthly average decrease of 10%. For land use change scenarios, agricultural development scenario indicated an opposite direction of changes in orthophosphate (increases in all months with an average increase of 6% under agricultural development scenario), leading to the conclusion that land use change is the dominant factor in nutrient concentration changes. Combined impacts results indicated that streamflows in late fall and winter months increased while in summer and early fall decreased. Suspended sediment and orthophosphate concentrations were decreased in all months except for increases in suspended sediment concentrations in September and October and orthophosphate concentrations in late winter and early spring due to the impact of land use change scenarios.

Keywords Climate change · Land use change · Hydrological modeling · Water quality · Kor River · Iran

Introduction

The positive and negative impacts of global climate change on the natural and social environment are confirmed by Intergovernmental Panel on Climate Change (IPCC). Changes in precipitation, temperature and sea level rise over the next century are predicted (Whitehead et al. 2015). In addition to climate change, land use activities such as conversion of natural landscapes for human use and different land management practices have transformed a large proportion of the earth's land surface. Deforestation, intense agricultural activities and urban area expansion in a watershed can influence different processes, including infiltration, groundwater recharge, baseflow and runoff (Fan and Shibata 2015).

Both of the climate and land use changes can affect water quantity and quality at different scales around the world (Praskievicz and Chang 2011). Because of the significance of their impacts on water resources, many researchers are interested in studying separate and combined effects of these two variables in order to manage water resources sustainably (Praskievicz and Chang 2009). Erosion and sediment transport processes also influenced by climate and land use change. For example, regions with the strong variability of precipitation and runoff are more

✉ Amir Asadi Vaighan
amir.vaigan@gmail.com; amir.vaighan@shirazu.ac.ir

Nasser Talebbeydokhti
taleb@shirazu.ac.ir

Alireza Massah Bavani
armassah@ut.ac.ir

[1] Department of Civil and Environmental Engineering, Faculty of Engineering, Shiraz University, Zand Street, Shiraz, Fars, Iran

[2] Department of Irrigation and Drainage Engineering, College of Abouraihan, University of Tehran, Pakdasht, Iran

Published online: 08 August 2017

susceptible to soil loss by erosion (Fan and Shibata 2015). Urbanization, agricultural development, mineral extraction and dam construction are the forms of land use change which can affect erosion and sediment transport processes (Shrestha et al. 2013).

A number of studies have addressed only the impacts of climate change on water quantity and/or quality (Abbaspour et al. 2009; Cox and Whitehead 2009; Rehana and Mujumdar 2011; Jin et al. 2012; Ficklin et al. 2013; Li et al. 2016; Praskievicz 2016). For instance, Jin et al. (2012) indicated that during the 2020s, drier hydrological conditions will prevail in the River Thames Catchment in southern England. The degree of dryness will be much more profound at the 2080s. Furthermore, their results showed that river NO_3–N concentration will increase in winter and decrease in summer as a result of climate change. There have also been several studies utilizing land use change impacts, and many of these consider the separate impacts of climate and land use changes (Tu 2009; Hadjikakou et al. 2011; Praskievicz and Chang 2011; Wilson and Weng 2011; Astaraie-Imani et al. 2012; Tong et al. 2012; Crossman et al. 2013; Kim et al. 2013; Mitsova 2014; El-Khoury et al. 2015; Fan and Shibata 2015; Pervez and Henebry 2015; Whitehead et al. 2015; Fernandes et al. 2016). For example, Fan and Shibata (2015) found that climate change scenarios have a greater impact in increasing surface runoff, lateral flow, groundwater discharge and water yield than land use change. They also confirmed that the sediment and nutrient loads were mainly supplied from agricultural land under land use in each climate change scenario, suggesting that land use change was responsible for nutrient and sediment load changes in the watershed. Some studies have investigated combined impacts of these two variables (Tu 2009; Praskievicz and Chang 2011; Wilson and Weng 2011; Tong et al. 2012; Kim et al. 2013; El-Khoury et al. 2015; Mehdi et al. 2015). Since both soil erosion and sediment delivery to river channels are affected by climate and land use changes, it is important to examine the potential impacts of these changes at the watershed scale. Some studies have investigated these impacts in different watersheds around the world (Albek and Albek 2003; Thodsen et al. 2008; Ward et al. 2009; Ficklin et al. 2013; Mukundan et al. 2013; Shrestha et al. 2013; Rodriguez-Lloveras et al. 2016; Praskievicz 2016).

Many researchers used Coupled Model Intercomparison Project Phase 3 (CMIP3) under Special Report on Emission Scenarios (SRES) in the IPCC Fourth Assessment Report (AR4). Only a few studies focused on the CMIP5 models based on Fifth Assessment Report (AR5) of the IPCC scenarios (Kim et al. 2013; Fernandes et al. 2016). In comparison with CMIP3, CMIP5 includes more comprehensive models and enhanced experiments. In addition, in CMIP5 higher-spatial-resolution models with a richer set of output fields are used. Compared to CMIP3, better documentation of the models and experiment conditions is provided for CMIP5 (Taylor et al. 2012). New scenarios called representative concentration pathways (RCPs) are based on greenhouse gas concentrations and emissions pathways. The RCPs also included impacts caused by land use changes. In contrast, the SRES scenarios were based on forcing by greenhouse gas and aerosol from artificial climate change factors (Kim et al. 2013). This research examines the separate and combined impacts of future climate change (near future 2020–2049) and land use change on streamflow, suspended sediment, total ammonia and phosphorus in Kor River Basin, Southwest of Iran, using CMIP5 model and new RCP scenarios.

Methods

Study area

Kor River is located in Maharloo-Bakhtegan Basin in the Fars Province (Southwest of Iran). Maharloo-Bakhtegan covers an area of about 31,874 km^2 which is 1.9% of the total area Iran. Kor River is the most important river in Maharloo-Bakhtegan Basin. Doroudzan dam was built in Kor River for optimum use of water (Fig. 1). The 960 million cubic meters of dam reservoir is used for electricity production, agriculture and industry in the region. Therefore, Kor River plays an important role in agro-economy and people's livelihood in the basin (Mohsenipour et al. 2013).

Kor River originates from the Zagros Mountains flows for 280 km before reaching the Bakhtegan Lake (Fig. 1). The total drainage catchment of the Kor River is 9700 km^2. Average annual temperatures and precipitations in the basin are 17 °C and 240 mm. Kor River starting from downstream of Doroudzan reservoir to Polekhan hydrometric station (1700 km^2) considered as a study area (Fig. 1). General characteristics of the selected area are summarized in Table 1. Two meteorological and hydrometric stations in the area are Doroudzan, Takhtejamshid, and Doroudzan, Polekhan, respectively. The majority of the inhabitants are employed in agriculture, with water from the river being predominantly used for irrigation. Industrialization, urbanization and intensive agricultural activities in the area led to increases in the concentration of nutrients, biochemical oxygen demand (BOD) and turbidity mainly due to the intensified use of mineral fertilizers (Fakhraei 2009). Wheat, rice and barley are the major crops in the area. As in 2008, average utilization rate of phosphate and nitrogen fertilizers was about 184 and 342 kg/hec/year.

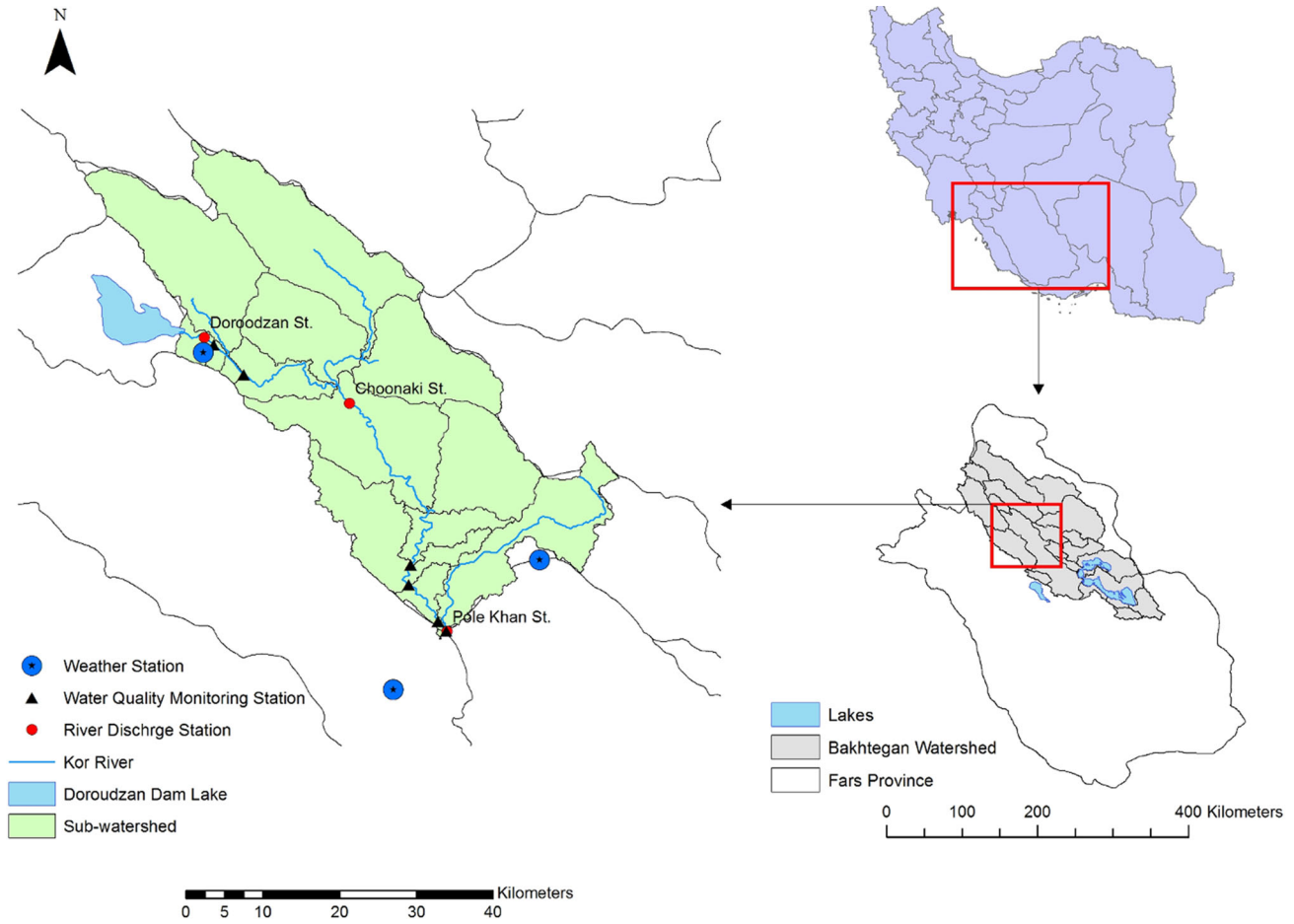

Fig. 1 Location of Kor River Basin in Fars Province, Iran

Table 1 General characteristics of the study area

Characteristic	Value
Area (km^2)	1700
Mean elevation (m)	1620
Average temperature (°C)	17
Average annual rainfall (mm)	240
Land use group	Percent (%)
Urban	1.4
Agriculture	39.5
Forest	16.3
Grassland	41.5
Rock	1.3

BASINS and WinHSPF model

An integrated environmental analysis system (BASINS) is developed by the EPA in 1994 for use in evaluating total maximum daily loads of pollutants and simulating hydrological impacts of management decisions (Praskievicz and Chang 2011). BASINS includes a number of sub-models, the most important of which is the Windows-based Hydrologic Simulation Program-Fortran (WinHSPF). WinHSPF is a robust, reliable and comprehensive model applied to flood forecasting, water quality modeling, as well as an assessment of best management practices and sensitivity of streamflow to climate change (Tong et al. 2012). As a lumped conceptual hydrological model, it represents physical process based on idealized system behavior and reports output for entire watershed defined by user-specified points. Water balance is calculated for selected points based on inputs of precipitation and different land uses. To calculate runoff on pervious and impervious land surfaces, separate water balance equations are used by WinHSPF (Praskievicz and Chang 2011).

Necessary time series for running WinHSPF are hourly scale meteorological data. Minimum hourly data required are precipitation and evapotranspiration data; however, other meteorological variables including maximum and minimum temperatures, wind speeds and cloud cover can also be included (Praskievicz and Chang 2011).

PERLND is the module of WinHSPF that simulates pervious land hydrology. Several dozen parameters that determine hydrological behavior are initially estimated by WinHSPF based on basin's climatic, topographic and land cover characteristics, then adjusted manually or automatically to optimize model performance (Praskievicz and Chang 2011; Tong et al. 2012). Lower and upper zone soil moisture storage, soil infiltration rate, length and slope of overland flow path, groundwater and interflow recession rates, evaporation coefficients, groundwater zone partitioning, vegetation interception and Manning's n roughness coefficient are some of the major adjustable parameters. The IMPLND module is used for impervious surfaces. RCHRES is the module for free-flow reaches in streams or lakes, each of which has different water balance equations for the calculation of flow and water quality (Praskievicz and Chang 2011; Tong et al. 2012).

In addition to hydrology simulation, sediment and nutrients mass balances are calculated by WinHSPF. In sediment processes, major adjustable parameters are coefficients for sediment wash off, soil matrix scours, solids wash off and solids accumulation rate. Nutrient loading, including total phosphorus, is another water quality constituent modeled by WinHSPF (Praskievicz and Chang 2011).

In WinHSPF, nutrient modeling for pervious and impervious land segments is modeled separately. For pervious land segments, two methods are used. The first method associates the accumulation and removal of the constituents with the overland flow. WinHSPF uses this method for modeling (NO_3) and ammonia (NH_4) since they are not adsorbed by sediment. The second method is the potency factor approach which relates constituent wash off to sediment removal and transport. This method is used for orthophosphate modeling since orthophosphate loads are associated with sediment loads (Bicknell et al. 2001).

For nitrate and ammonia simulation, the following equation is used (Bicknell et al. 2001):

$$C_{\mathrm{w}} = C_{\mathrm{S}} \times (1 - \mathrm{e}^{-Q_{\mathrm{s}} \times S_{\mathrm{c}}}) \quad (1)$$

where C_{w} is the quality constituent of wash off from land surface (quantity/ac/interval), C_{s} is the available quality constituent in storage (quantity/ac) and S_{s} is the susceptibility of the quality constituent to wash off (1/in).

The second method, which associates constituent wash off with sediment transport, is calculated by the following equation (Bicknell et al. 2001):

$$C_{\mathrm{w}} = S_{\mathrm{wo}} \times w_{\mathrm{c}} + C_{\mathrm{sc}} \times f_{\mathrm{s}} \quad (2)$$

where C_{w} is the total flux of constituent from land segment associated with the sediment runoff (quantity/ac/interval), S_{wo} is the detached sediment wash off (tons/ac/interval) calculated in sediment simulation step, w_{e} is the wash-off potency factor (quantity/ton), C_{sc} is the scour of matrix soil (ton/ac/interval) and f_{s} is the scour potency factor (quantity/ton).

For an impervious land segment, wash off of quality constituents can also be calculated in two ways, similar to a pervious land segment. The first method associates wash off of constituent with overland and therefore uses the same equation as pervious land segment [Eq. (1)]. The second method attributes wash off of constituent with sediment wash off and is calculated by (Bicknell et al. 2001):

$$C_{\mathrm{w}} = S_{\mathrm{wo}} \times w_{\mathrm{c}}. \quad (3)$$

The scouring component was eliminated for impervious land segment since scouring is assumed not to be a factor.

This model was selected for this study for three primary reasons. First, BASINS has a large user community with an abundant case study and technical support. Second, Hydrological Simulation Program-Fortran (HSPF) has advantages over many other hydrological models. It simulates loadings of several water quality constituents in addition to hydrology, therefore allowing for comprehensive assessment of long-term impacts on both water quality and quantity. Finally, compared to Soil and Water Assessment Tool (SWAT), HSPF was developed for use in mesoscale, mixed land use basins (Praskievicz and Chang 2011).

Input data and model setup

Hydrometeorological data: WinHSPF requires hourly precipitation, minimum and maximum air temperature as a minimum required data. Evapotranspiration time series are calculated based on the daily minimum and maximum air temperatures and specific monthly coefficients using Hamon's potential evapotranspiration formula (Hamon 1961). This method generates daily potential evapotranspiration using air temperature (Fahrenheit or Celsius), a monthly variable coefficient, the number of hours of sunshine (computed from latitude) and absolute humidity (compute from air temperature) (Hamon 1961):

$$\mathrm{PET} = \mathrm{CTS} \times D_{\mathrm{YL}}^2 \times V_{\mathrm{DSAT}} \quad (4)$$

where PET is the daily potential evapotranspiration (inch), CTS is the monthly variable coefficient, D_{YL} is the possible hours of sunshine, in units of 12 h, computed as a function of latitude and time of year, and V_{DSAT} is the saturated water vapor density (absolute humidity) at the daily mean air temperature (g/cm^3) (Hamon 1961):

$$V_{\mathrm{DSAT}} = \frac{(216.7 \times V_{\mathrm{PSAT}})}{T_{\mathrm{Ave}} + 273.3} \quad (5)$$

where V_{PSAT} is the saturated vapor pressure at the air temperature, and T_{Aver} is the mean daily air temperature, computed from daily max–min data (°C) (Hamon 1961):

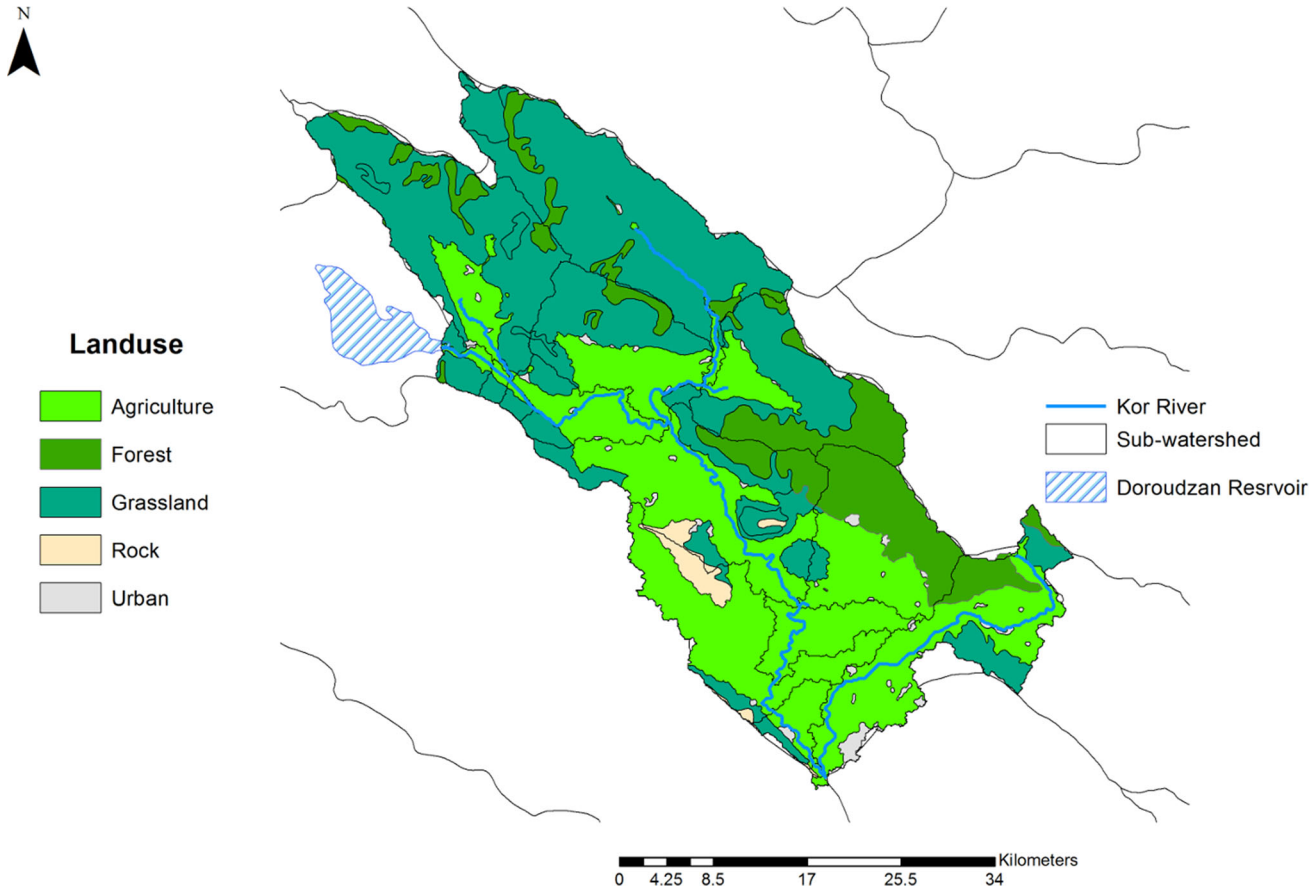

Fig. 2 Land use and land cover map of study area

$$V_{\mathrm{PSAT}} = 6.108 \times \mathrm{e}^{\left(\frac{17.26939 \times T_{\mathrm{Aver}}}{T_{\mathrm{Aver}} + 237.3}\right)}. \quad (6)$$

Hamon (1961) suggested a constant value of 0.0055 for CTS. However, this has found to underestimate PET in some areas, especially for winter months. Therefore, monthly values can be specified. The hourly observed precipitation and air temperature data (1988–2015) for two meteorological stations (Doroudzan and Takhtejamshid) (Fig. 1) in the study area were provided by the Fars Meteorological Research Organization.

Digital elevation model (DEM): The topographic data used in this study included elevation, slope, aspect, flow direction and accumulation. These data were obtained from a digital elevation model (DEM) with 30-m grid provided by US Geological Survey (USGS) Global Data Explorer. The DEM was used to delineate the watershed boundary, along with 16 subwatersheds as presented in Fig. 1. River networks, watershed boundaries and other geographical properties of the study area acquired from Fars Regional Water Authority.

Land use properties: In addition to weather information, WinHSPF requires land use and land cover information to simulate loads in the hydrological components. Land use data (Globcover 2009) were obtained from European Space Agency Globcover Portal (http://due.esrin.esa.int/page_globcover.php). 22 classes of Globcover 2009 were reclassified into 5 groups (Fig. 2).

Model calibration and validation

Model calibration and validation are necessary and critical steps in any model application. In order to calibrate HSPF, an iterative process of parameter adjustment is needed. This can be done by comparing simulated and observed values of interest. To adjust parameters under a variety of climatic, soil moisture and water quality conditions, several years of simulation (at least 3–5 years) are required. Model calibrated when the best overall agreement between simulated and observed values throughout the calibration period is achieved.

Hydrology calibration of HSPF precedes the sediment erosion and sediment transport and water quality calibration. In-stream hydraulics adjustment must be completed before in-stream sediment and water quality calibration due to the importance of transport mechanism of runoff. Model's validation purpose as an extension of the

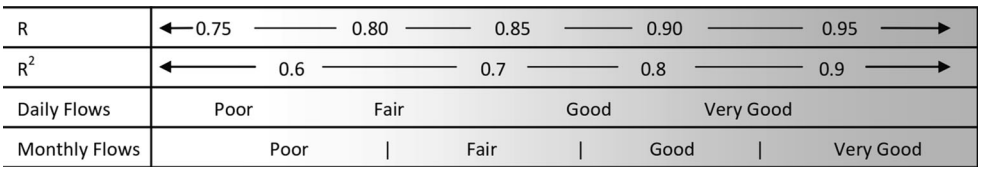

Fig. 3 R and R^2 value ranges for model performance (Duda et al. 2012)

Table 2 General calibration/validation targets or tolerances for HSPF applications (Duda et al. 2012)

	% Difference between simulated and observed values		
	Very good	Good	Fair
Hydrology/flow	<10	10–15	15–25
Sediment	<20	20–30	30–45
Water temperature	<7	8–12	13–18
Water quality/nutrients	<15	15–25	25–35
Pesticides/toxics	<20	20–30	30–40

calibration process is to ensure that calibrated model properly examines all the variables and conditions that can affect model results (Duda et al. 2012).

HSPF model's performance can be evaluated by coefficient of determination, R^2, one of the most commonly used statistical measures for model assessment. In addition, Nash–Sutcliffe model efficiency, NSE (Eq. 7) and the annual deviation of runoff volumes, or the percentage difference between modeled and observed annual flow volume (Eq. 8), can be used to evaluate the model's water balance (Duda et al. 2012).

$$\mathrm{NSE} = 1 - \frac{\sum(Q_{\mathrm{sim}} - Q_{\mathrm{obs}})^2}{\sum(Q_{\mathrm{obs}} - Q_{\mathrm{Aver}})^2} \tag{7}$$

$$\text{Percentage Difference} = \left(\frac{Q_{\mathrm{sim}} - Q_{\mathrm{obs}}}{Q_{\mathrm{obs}}}\right) \times 100 \tag{8}$$

where Q_{sim} is the simulated flow (m^3/s), Q_{obs} is the observed flow (m^3/s) and Q_{Aver} is the average daily flow (m^3/s). Suggested ranges of R, R^2 and percent difference between simulated and observed values are in Fig. 3 and Table 2.

HSPF can use Hydrological Simulation Program Expert (HSPEXP). The HSPEXP guides the modeler using expert advice compiled from experienced modelers. An acceptable HSPF calibration is achieved when the percent errors between the simulated and observed data are less than or equal to the limits set by the modeler (Kim et al. 2007). The HSPEXP decision-support software provides calibration guidance, suggesting parameter adjustments that, respectively, address total volume, the low flows, storm flows and finally seasonal flows (Kim et al. 2007).

In this study, WinHSPF run for the period of 2003–2012 at Polekhan station, at the end of the basin (Fig. 1). The 2003–2008 period served as the calibration period, and the 2009–2012 was the validation period. HSPEXP was used for calibration of hydrology. To evaluate the model's performance R^2, Nash–Sutcliffe model efficiency, (Nash and Sutcliffe 1970) and percent difference were used.

Climate change scenarios (CC)

In this research, the outputs of the fourth generation of The Community Climate System Model (CCSM4.0-AR5) developed by US National Center for Atmospheric Research were used as climate change scenarios. The outputs of the CCSM4.0 with a surface grid whose spatial resolution is 1.25° × 0.9° for four RCP scenarios were downloaded from the website of Center for Environmental Analysis (CEDA) (URL http://browse.ceda.ac.uk/browse/badc/cmip5/data/cmip5/output1/NCAR/CCSM4). The two scenarios are RCP 2.6 and RCP 8.5 (low- and high-limit scenarios), which were constructed to explore greenhouse gas concentration and emissions pathways. The monthly precipitation, minimum and maximum air temperatures and average temperatures for the historical period 1976–2005 and near-future period 2020–2049 were downloaded from the above-mentioned website.

The delta changes downscaling technique is a method that makes the output of GCMs useful for catchment-scale analysis and hydrological modeling. The method is based on the use of a change factor, the ratio between a mean value in the future and historical run (Ruiter 2012). In this research, changes in mean climate, for each calendar month, are calculated based on (Jones and Hulme 1996):

$$\Delta \mathrm{Ti} = \left(\bar{T}_{\mathrm{GCM,fut},i} - \bar{T}_{\mathrm{GCM,base},i}\right) \tag{9}$$

$$\Delta \mathrm{Pi} = \left(\bar{P}_{\mathrm{GCM,fut},i} / \bar{P}_{\mathrm{GCM,base},i}\right) \tag{10}$$

where ΔTi and ΔPi are the change in 30-year average for each month of temperature and precipitation for the

historical period (1976–2005) to a future period (2020–2049). $\bar{T}_{GCM,fut,i}$ and $\bar{P}_{GCM,fut,i}$ are 30-year average of temperature and precipitation of future period for each month. $\bar{T}_{GCM,base,i}$ and $\bar{P}_{GCM,base,i}$ are 30-year average of similar variables for each month of historical period. These changes then used in LARS-WG in order to generate future time series of temperature and precipitation of Doroudzan and Takhtejamshid stations (Fig. 1). LARS-WG is a stochastic weather generator which can be used for the simulation of weather data at a single station under both current and future climate conditions (Etemadi et al. 2012). Produced time series then are used in WinHSPF in order to evaluate climate change impacts on streamflow, suspended sediment and water quality of Kor River Basin.

Land use change scenarios (LC)

Based on previous research, agricultural land in the area in 2008 was 1.6 times in comparison with 1956 (Royan Consulting 2008). This trend is assumed to continue in the future. Three future land use change scenarios (LC) were set up: (1) constant (LC) will not change; the current land data (2009) will be used for the future period (Baseline), (2) agricultural development; agricultural land use will increase by 60% (LC 60) relative to baseline, (3) urban development; urban land use will increase by 30% (LC 30) relative to baseline. In order to increase agricultural land use by 60% (LC 60) or urban land use by 30% (LC 30), other land use types will remain constant and second dominated land use category in the study area (grassland land use) will decrease in sub watersheds. Land Use Editor tool in WinHSPF was used to apply each land use scenario by adding or subtracting desired land use types in each reaches. Then, WinHSPF calculates a water balance for each reach based on inputs and hydrological parameters for different land cover classes. WinHSPF uses separate water balance equations to calculate runoff on pervious and impervious land surfaces. After hydrology simulation, the total sediment outflow is calculated by adding sediment outflow from pervious land segment with sediment outflow from the impervious land segment. Nutrient modeling for pervious and impervious segments is modeled separately using two methods. The first method associates the accumulation and removal of constituents with the overland flow (NO_3 and NH_4). The second method is the potency factor approach which relates constituent wash off to sediment removal and transport (PO_3) (Bicknell et al. 2001).

Combined scenario setup

In this study, three different scenarios (climate change, land use change and combined climate and land use change) were defined to evaluate the separate and combined impacts on streamflow, suspended sediment and water quality. Combined scenarios were set up: (1) High climate change (RCP 8.5)—Agricultural development (HCC-LC60), 2) Low climate change (RCP 2.6)—Agricultural development (LCC-LC60), (3) High climate change (RCP 8.5)—Urban development (HCC-LC30), (4) Low climate change (RCP 2.6)—Urban development (LCC-LC30). The simulated streamflow suspended sediment concentration and water quality constituent concentration for the future period (2020–2049) were compared to the corresponding values for the baseline period (2003–2012).

Results and discussion

Calibration and validation results

The HSPF model was calibrated and validated for streamflow, sediment and water quality simulations. Several model parameters included in WinHSPF calibration of flow, sediment and water quality (Table 3). The model was calibrated for 2003–2008 and validated for 2009–2012 at Polekhan stream discharge station along the Kor River watershed using the 2009 land use. To evaluate model's goodness of fit, the coefficient of determination or R^2, Nash–Sutcliffe model efficiency, NSE (Nash and Sutcliffe 1970) and percent difference between modeled and observed were used. Table 4 shows the summary statistics for calibration and validation. The model was considered as "Good" for values of R^2 and percent differences (Fig. 3; Table 2). Observed and simulated time series of streamflow, suspended sediment, total ammonia and orthophosphate in calibration and validation periods are presented in Fig. 4a, b. The results show that the calibrated model can describe the streamflow, sediment and water quality in the Kor River Basin and confirm that the calibrated model with optimized parameters can be applied to determine the basin's responses to climate and land use changes.

Impact of future climate change

In order to assess the climate change impacts on streamflow, suspended sediment and water quality, it is necessary to evaluate future changes in precipitation and temperature. Future climate projections based on two RCP scenarios (RCP 2.6 and RCP 8.5) of 2020–2049 future period were compared to baseline climatology (temperature and precipitation for 1988–2015) for Doroudzan station. Figure 5 shows the change in average monthly temperature and precipitation compared to baseline 1988–2015 period. According to Fig. 5, temperature increases in all months except in January for RCP 8.5, higher in magnitude

Table 3 Initial and final values of calibrated hydrology, sediment and water quality parameters for the Kor River Basin

Category	Parameter	Description	Unit	Recommended range	Initial value	Final value
Hydrology	LZSN[a]	Lower zone nominal soil moisture storage	mm	76.2–203.2	152.4–165.1	76.2–88.9
	INFILT	Index to infiltration capacity	mm/h	0.254–6.35	4.06	0.635–1.52
	AGWRC	Base groundwater recession	Ratio	0.92–0.99	0.98	0.98
	INTFW	Interflow inflow parameter	None	1.0–3.0	0.75	5.5
	DEEPFR	Fraction of groundwater inflow to deep recharge	Ratio	0.0–0.2	0.02	0.0
	BASETP	Fraction of remaining evapotranspiration from baseflow	Ratio	0.0–0.05	0.02	0.0
	IRC	Interflow recession parameter	None	0.5–0.7	0.7	0.85
	Month UZSN	Monthly upper zone nominal storage	mm	2.54–25.4	0.0	8.38–13.97
	Month Manning's n	Monthly Manning's n	None	0.05–0.5	0.0	0.01–0.09
	Month LZETPARM	Monthly lower zone E-T parameters	None	0.2–0.7	0.0	0.2–0.7
Sediment	MON-COVER	Monthly vegetation cover	None	0.25–0.95	0.5	0.25–0.95
	KRER	Soil detachment coefficient	None	0.15–0.45	0.3	10
	JRER	Soil detachment coefficient exponential	None	1.0–3.0	2	1
	KSER	Sediment wash-off coefficient	None	0.1–10	0.25–1.2	4–10
	JSER	Sediment wash-off coefficient exponential	None	1.0–3.0	2	2
	AFFIX	Daily detached sediment reduction rate	1/day	0.03–0.1	0.2	0.002–0.01
	ACCSDP	Solids accumulation rate on impervious land surface	tons/acre/day	0.0–2.0	0.01	0.03
	TAUCS-SILT	Critical shear stress for silt scour	tons/acre	0.2–65.4	0.32	16.33
	TAUCD-SILT	Critical shear stress for silt deposition	tons/acre	0.02–21.78	0.1	9.80
	TAUCS-CLAY	Critical shear stress for clay scour	tons/acre	0.2–65.4	0.3	17.42
	TAUCD-CLAY	Critical shear stress for clay deposition	tons/acre	0.02–21.78	0.06	10.01
Water quality	IOQC	Constituents concentration in interflow outflow	mg/l	None	0.0	0.01
	AOQC	Constituents concentration in groundwater outflow	mg/l	None	0.0	0.01–0.015
	MON-ACCUM	Monthly rate of accumulation	None	None	0.003–1.05	0.003–1.05
	MON-SQOLIM	Monthly storage rate	None	None	0.004–3.16	0.004–3.16
	POTFW	Potency factor[b]	None	None	0.0	0.59
	KTAM20	Oxidation rate of total ammonia	1/hr	0.001–0.4	0.015	0.03
	KNO320	Denitrification rate of nitrate	1/hr	0.001–0.4	0.002	0.4

[a] LZSN varies according to land use category

[b] Potency factor only applied to sediment attached constituent (ortho P)

particularly in the summer. The precipitation was predicted to increase significantly in autumn and winter months and slightly in winter and spring and summer months (except for August). Average temperature increases were 0.52 and 0.63 °C under RCP 2.6 and RCP 8.5, respectively. The maximum increase in average temperature was 0.9 °C under RCP 8.5 in July. Furthermore, maximum increase and decrease in precipitation were 421 and 85% under RCP 2.6 in September and August, respectively.

The simulated results of the streamflow, suspended sediment concentration, ammonia and orthophosphate concentrations (for the future period 2020–2049 relative to the baseline period (2003–2012) are shown in Fig. 6. There were some differences between two scenarios. However, in general, streamflow was predicted to increase significantly in October–February and slightly in March–September (Fig. 6a). The differences between these two scenarios originated from their difference in precipitation and temperature projections. In particular, the streamflow increases by 52% under RCP 2.6 in December but increased by 170% under RCP 8.5. Meanwhile, the streamflow decreases by 3% in April under RCP 2.6 and increases by 7% under RCP 8.5. The seasonal streamflow shows the impacts of future climate change more clearly than monthly

Table 4 Summary of calibration and validation statistics for Kor River Basin at Polekhan hydrometric station

Parameter	Run	Calibration			Validation		
		R^2	NSE		R^2	NSE	
Flow	Initial daily	0.70	0.49		0.69	0.46	
	Final daily	0.88	0.77		0.9	0.81	
	Final monthly	0.97	0.94		0.98	0.96	
Sediment	Daily	0.87	0.80		0.83	0.32	
Ammonia	Daily	0.82	0.80		0.79	0.60	
Orthophosphate	Daily	0.83	0.81		–[a]	–[a]	
Measures	HSPEXP performance criteria (%)	Observed	Simulated	Error (%)	Observed	Simulated	Error (%)
Total runoff (in.)	10	123.18	124.89	1.39	23.08	25.20	9.18
Total of highest 10% flows (in.)	15	7.77	7.27	−6.38	11.75	12.13	3.23
Total of lowest 50% flows (in.)	10	3.13	3.35	6.87	0.462	0.485	4.97
Seasonal volume error (%)	20	NaN	NaN	−1.02	NaN	NaN	−12.3
Winter flow volume (in.)	NaN	6.29	6.42	1.95	2.27	2.56	12.77
Summer flow volume (in.)	NaN	3.45	3.48	0.93	1.17	1.39	18.80

[a] No data available in validation period

streamflow (Kim et al. 2013). According to their results, the general pattern indicated increases in spring and summer flow and decreases in autumn flow. This is different from our result which showed significant increases in autumn and winter and slight increases in spring and summer. This difference can be explained by the different precipitation patterns in the Hoeya River Basin which had low monthly precipitation from October to January and rainy season with typhoons from February to September. In contrast, Kor River Basin had larger precipitations from October to January and low precipitations from March to September. These trends of streamflow change were similar to study carried out by Praskievicz and Chang (2011) under CCSM3.0 B1 and CCSM3.0 A1B scenarios which experienced a wet, mild winter and dry warm summer.

Projected sediment concentrations showed a monthly average of 10% decrease with the maximum of 37% under RCP 8.5 (Fig. 6b). Suspended sediment concentrations decreased moderately in all months except for September and October (9.5 and 3.3% increase under RCP 2.6). According to Ficklin et al. (2013), the reduction in sediment concentration was not well understood. However, decreases in sediment concentration are mostly attributed to changes in hydrology. Streamflow and surface runoff changes could play important roles in sediment concentration. Less energy due to decreased streamflow will result in less sediment transport capacity. Alternatively, decreased surface runoff will result in less energy and capacity to transport sediment. In another study by Wilson and Weng (2011), TSS concentration was not linearly related to streamflow under certain climate change scenarios. TSS concentration may be lower than baseline period while predicted loads were higher than the baseline period.

As shown in Fig. 6c, ammonia concentrations were decreasing all months with more decreases during winter and spring months (maximum values of 24 and 41% decrease in December under RCP 2.6 and RCP 8.5, respectively). This can be attributed to sharp increases in streamflows during winter and spring months and relatively slight increases during summer months which leads to more dilution potential during these periods under two scenarios. Effects of dilution on ammonia concentration decreases during wet months have confirmed by previous studies (Whitehead et al. 2002, 2006; Hadjikakou et al. 2011; El-Khoury et al. 2015). They indicated that increased flows mainly lead to increase in dilution potential which could decrease nitrogen concentrations (Hadjikakou et al. 2011).

Changes in orthophosphate concentrations are closely related to flow and sediment concentration (Praskievicz and Chang 2011). According to Fig. 6d, there are decreases in all months for both climate change scenarios. The maximum decrease in orthophosphate concentration was 40% in December under RCP 8.5, and the minimum decrease was 0.22% in September under RCP 2.6. The average annual decrease for RCP 2.6 was 10%, and the average decrease for RCP 8.5 was approximately 16%. As previously mentioned, orthophosphate modeled as a function of sediment load in BASINS–WinHSPF. Therefore, it is easily adsorbed to the sediment (Praskievicz and Chang 2011). As our study results suggested, by nearly same

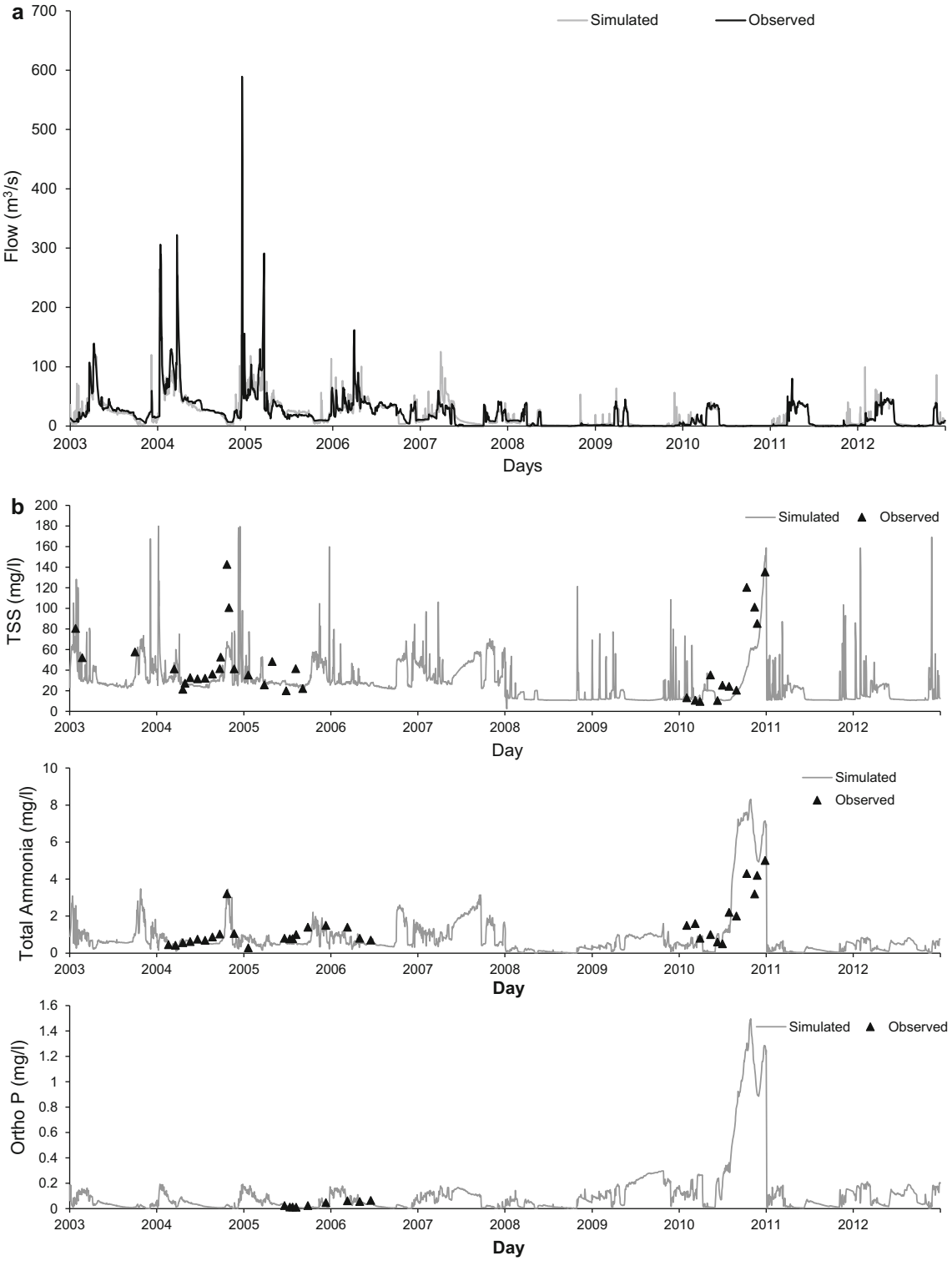

Fig. 4 **a** Observed and simulated daily flow for Kor River at Polekhan hydrometric station, calibration (2003–2008), validation (2009–2012). **b** Observed and simulated daily suspended sediment, total ammonia and orthophosphate for Kor River at Polekhan hydrometric station, calibration (2003–2008), validation (2009–2012)

pattern, decreasing suspended sediment concentration, leads to a decrease in orthophosphate concentration (Fig. 6b, d). According to Praskievicz and Chang (2011), there is a strong relationship between flow, sediment and orthophosphate load and concentration. Orthophosphate is highly attracted to soil particles and so is highly correlated

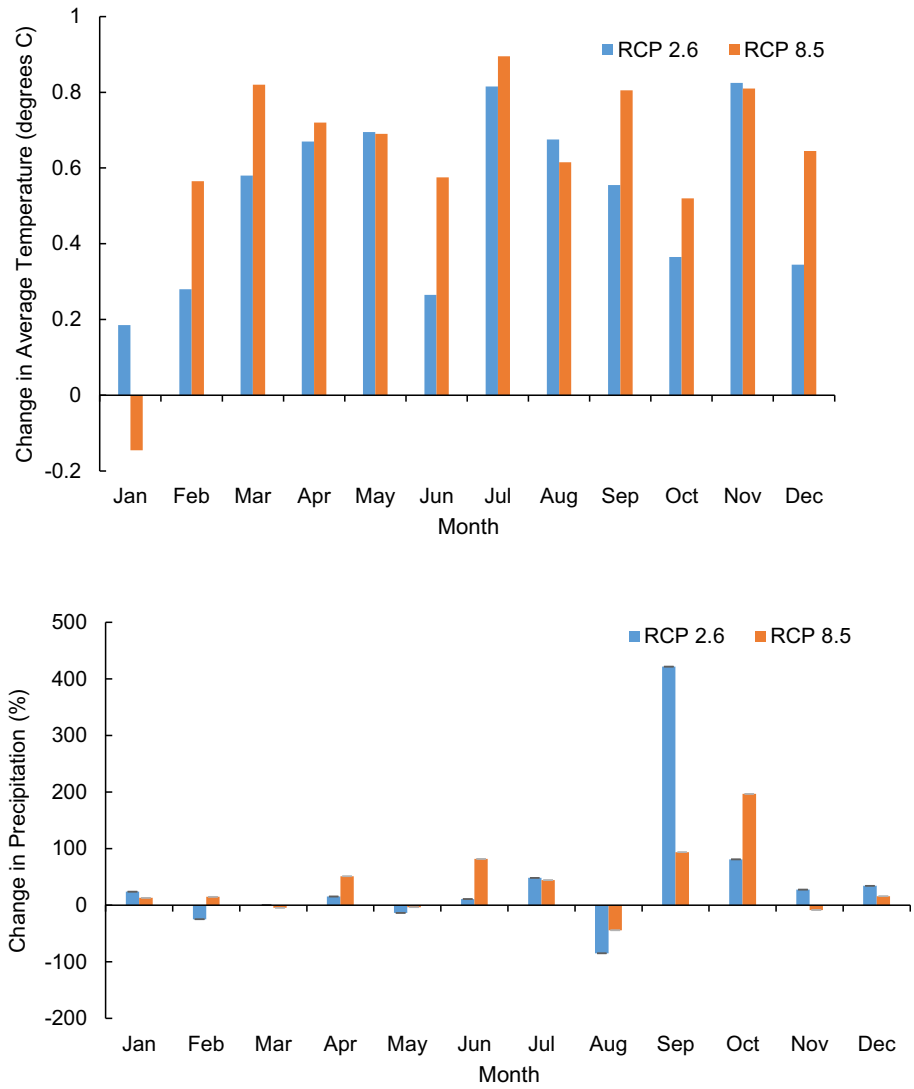

Fig. 5 Change in average monthly temperature and percentage changes in total monthly precipitation from baseline (1988–2015) for the 2020–2049 under two climate change scenarios

to sediment. Other studies (Wilson and Weng 2011; Tong et al. 2012; Fan and Shibata 2015) also reported that the phosphorous is attached to suspended sediment and changes in suspended sediment concentration would directly affect the phosphorous concentration.

Impacts of future land use change

Water resources quantity and quality are widely affected by land use changes such as urban growth and agricultural development. Figure 7 represents changes in monthly streamflows, suspended sediment, total ammonia and orthophosphate concentrations for two future land use change scenarios. Little changes in streamflow compared to climate change scenarios were observed (Fig. 7a). Under agricultural development scenario (LC60), streamflows decreased from January to September and increased from October to December. Furthermore, under urban development scenario (LC30) approximately no changes in streamflow were predicted except for winter months with a maximum increase of 0.3% in December. Maximum increase and decrease in streamflow changes for LC60 were 3 and 2.7% in December and April months, respectively. As previously mentioned, Kor River Basin was an agricultural-dominated watershed (with mean monthly precipitation 78–120 mm from October to February (rainy season) and major crop growing season October to May); thus, future changes in agricultural land use would affect streamflows more than urban development. Agricultural development in the watershed will increase pervious surface cover, increase infiltration and hence decrease runoff. In contrast, as with urban development in the basin, precipitation infiltration will decrease and runoff will increase as a result of an impervious surface cover increase (Kim et al. 2013). Reductions in streamflow caused by urban growth have been reported by previous studies (Tu 2009;

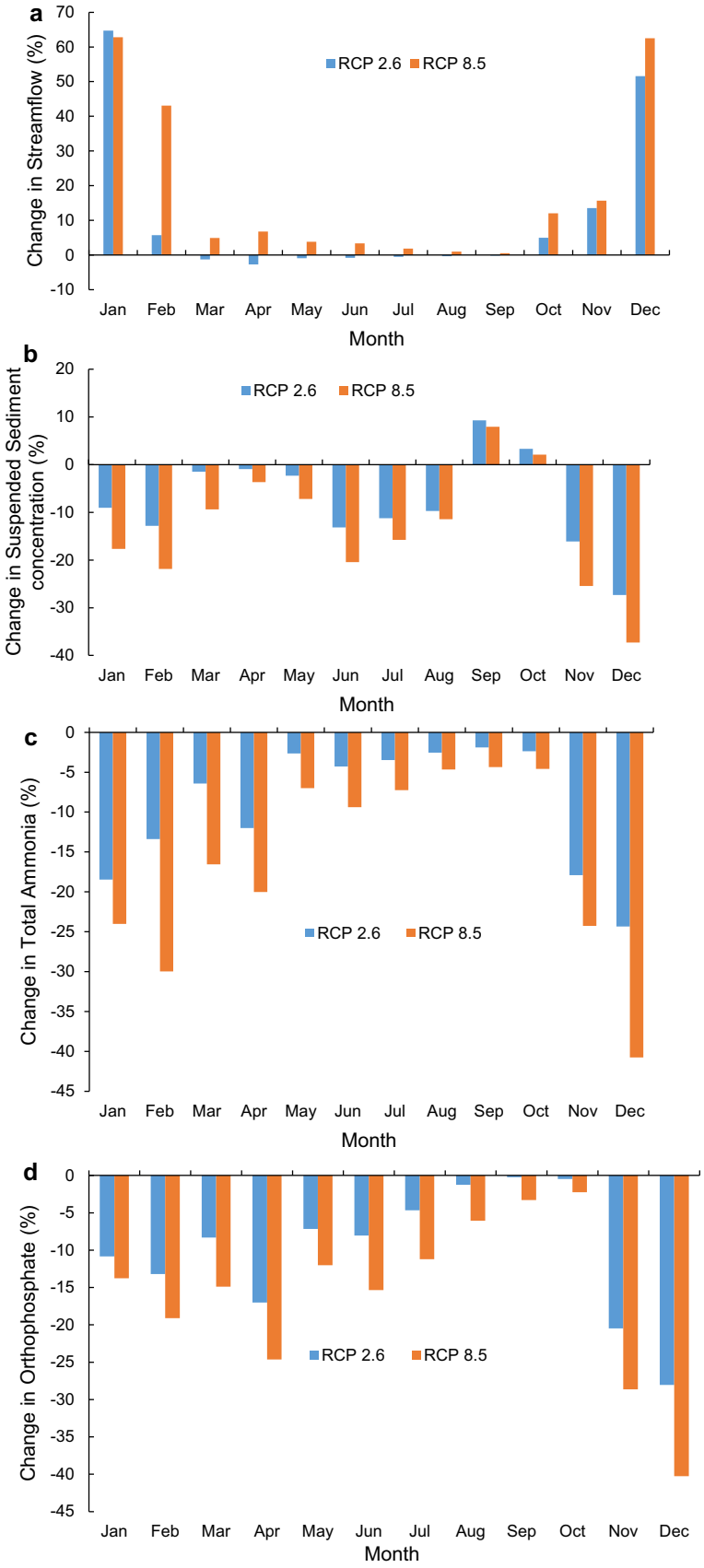

Fig. 6 Change in **a** streamflow, **b** suspended sediment, **c** total ammonia, **d** orthophosphate concentration in the future period (2020–2049) relative to the baseline (2003–2012) under climate change scenarios

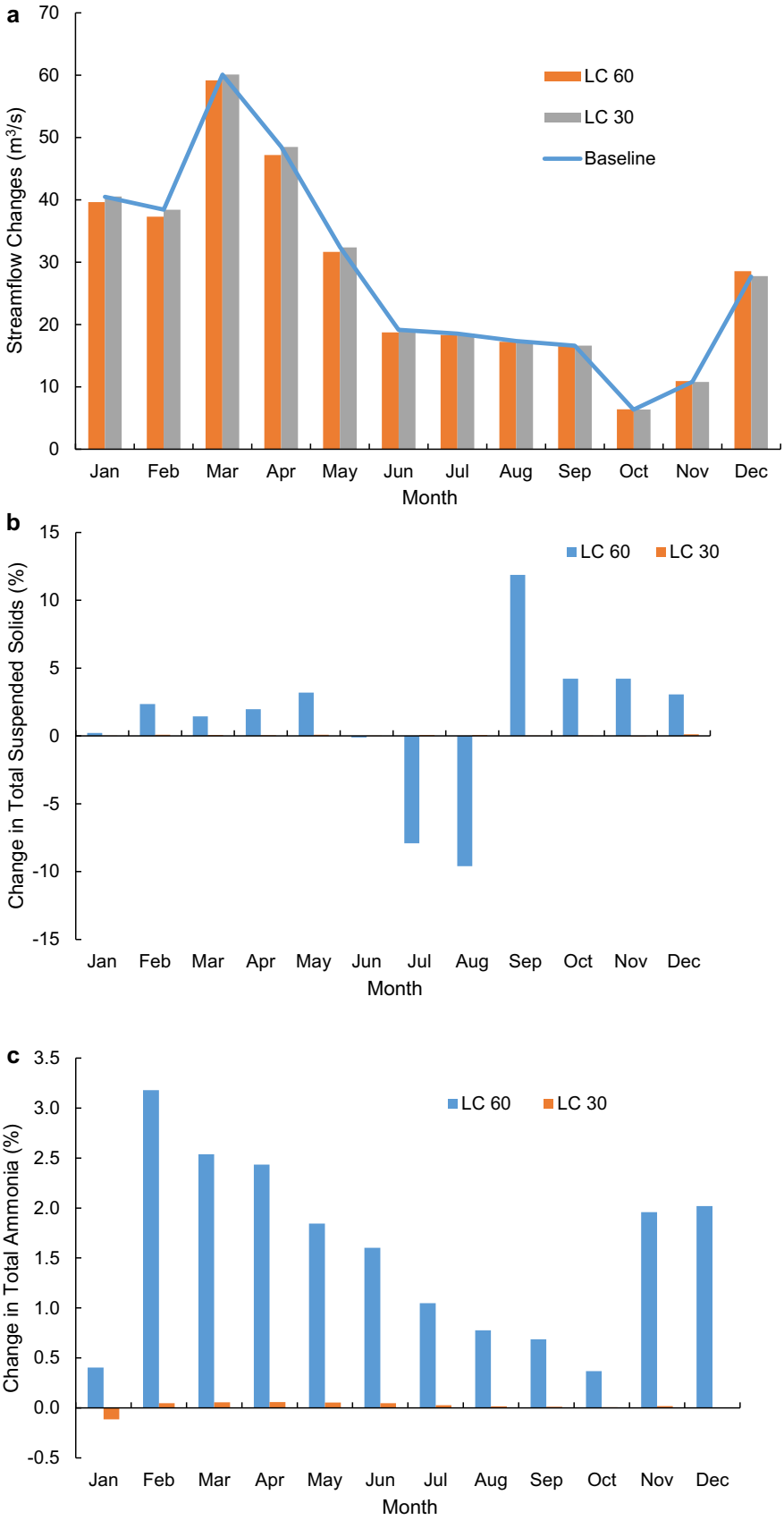

Fig. 7 Change in **a** streamflow, **b** suspended sediment, **c** total ammonia, **d** orthophosphate concentration in the future period (2020–2049) relative to the baseline simulations (2003–2012) under land use change scenarios LC60 = 60% increase in agricultural land use, LC30 = 30% increase in urban land use, **a** shows the mean monthly streamflow values for the baseline (2003–2012) and two land use change scenarios (LC60 and LC30), **b**–**d** show the percent change (%) in TSS, total ammonia and ortho P relative to baseline. **e** Shows the mean monthly load values of total ammonia under two land use change scenarios relative to baseline

Fig. 7 continued

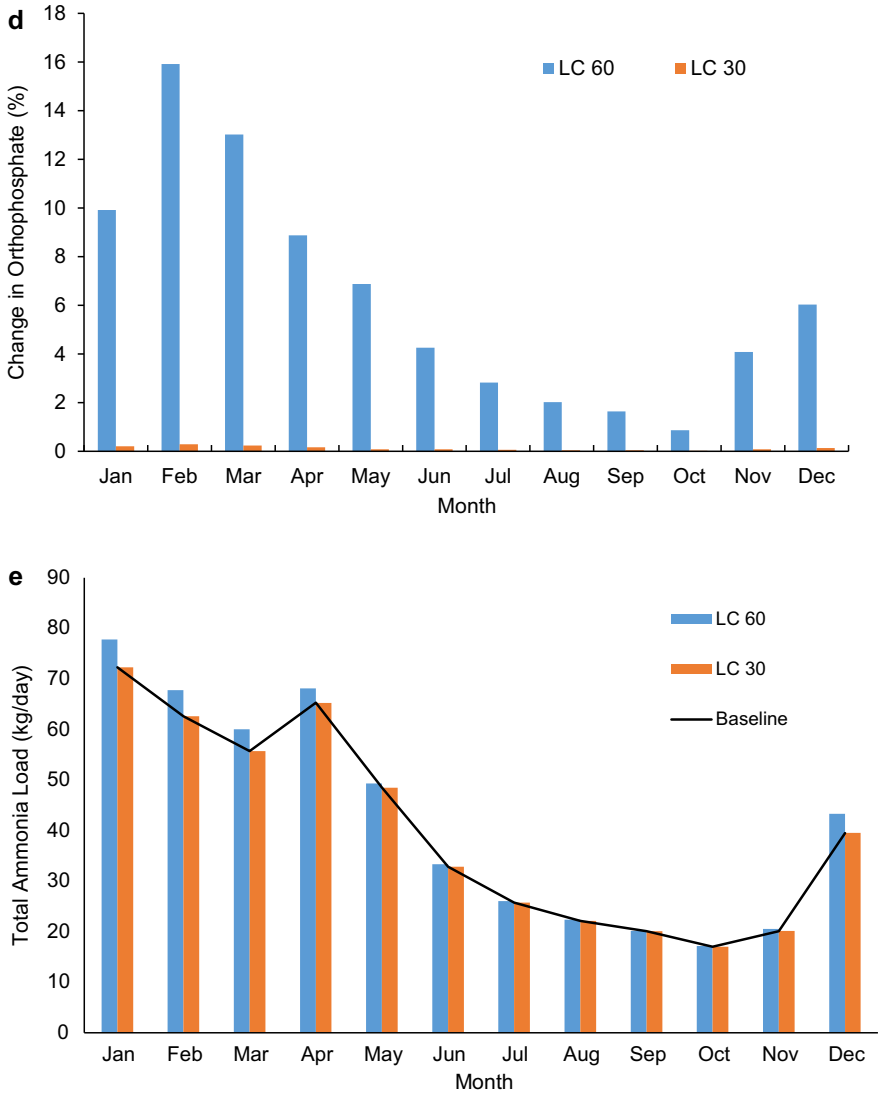

Praskievicz and Chang 2011; Dixon and Earls 2012; Tong et al. 2012; Pervez and Henebry 2015).

As with streamflow responses to land use scenarios, the magnitude of changes in suspended sediment concentrations was lower than climate change scenarios. Suspended sediment concentrations were increased under LC60 scenario and approximately were constant under LC30 (Fig. 7b). The maximum increase in suspended sediment concentration was about 12 and 10% in September and August for LC60, respectively. As expected, Kor River Basin was less sensitive to urban development due to its dominant agricultural land use, and as a result, nearly no change was observed in suspended sediment concentrations under LC30. Praskievicz and Chang (2011) reported that urban development will result in higher suspended sediment load in the highly urbanized watershed. Wilson and Weng (2011) also stated that land use composition and relatively flat topography could affect runoff and increase TSS load and as a result TSS concentration levels.

Land use change impacts on total ammonia and orthophosphate concentrations were investigated (Fig. 7c–e). According to the results, ammonia and orthophosphate concentrations were increased in all months for agricultural development scenario (LC60) compared to LC30 which nearly no change occurred. This can be expected, as with agricultural growth more fertilizers will be applied to the land and as a result more ammonia and phosphorous will be washed off or infiltrated to the stream by irrigation. Tu (2009) has been reported that nutrients are mostly affected by agricultural activity in less urbanized areas. Therefore, nitrogen concentration increases might be associated with land development in watersheds. Furthermore, Tu and Xia (2008) reported that in less urbanized watersheds, the impact of land use change on water quality is higher than

highly urbanized watersheds. El-Khoury et al. (2015) have confirmed that in agricultural-dominated watershed land development is the primary source of nutrient concentrations changes. In addition, results of their study showed that magnitude of climate and land use change impacts is not the same and varies according to the water quantity and quality parameters.

Combined impacts of climate and land use change

Combined impacts of climate and land use change were evaluated and are presented in Fig. 8. As Fig. 8a indicates, streamflows in late fall and winter months (October through February) increased while the streamflows in summer and early fall (June through September) decreased or not changed. The pattern of streamflow changes was similar to climate change scenarios with greater in magnitude under combined scenarios. Scenarios with high climate change (HCC) showed more increases relative to low climate change scenarios (LCC). Additionally, under urban development scenarios (LC30), the magnitude of changes was greater than agricultural development scenarios (LC60). This can be explained by the contribution of high climate change and urban development. When these scenarios occur simultaneously, reduced infiltration of precipitation due to increased impervious surface areas and precipitation under high climate change scenarios can enhance streamflows. Streamflow sensitivity to climate change rather than land use change has been confirmed by previous studies (Tu 2009; Praskievicz and Chang 2011; Tong et al. 2012; Kim et al. 2013; El-Khoury et al. 2015; Fan and Shibata 2015). Moreover, Praskievicz and Chang (2011) stated that combined change scenarios predicted a higher increase in winter flows than the climate change. They also pointed out that in combined scenarios larger changes in streamflow were due to the contribution of impervious urban surfaces which reduce infiltration of precipitation and increase runoff compared to climate change scenarios. When climate change and land use change occur simultaneously, change in streamflow for all months is enhanced (Tu 2009).

Figure 8b shows the predicted changes in suspended sediment concentration under combined scenarios. Concentrations decrease in all months except for an increase in September and October under all scenarios. Combined scenarios with high climate change generally have greater impacts on suspended sediment concentrations than either of low climate change scenarios. Under high climate change scenarios, the maximum decrease in suspended sediment concentration was 37% in December under HCC-LC30. The maximum increase in TSS concentration was 11% in September under LCC-LC60. In comparison with climate change scenarios in which maximum decrease and increase were 37 and 9.3% under RCP 8.5 and RCP 2.6, approximately no contribution of land use change scenarios on TSS concentration change was observed. The model result indicated that climate change might be more important than land use change in future sediment dynamics in the Kor River Basin. Moreover, our results indicated that TSS concentration is not always linearly related to river discharge as, under climate scenarios, TSS concentration can be lower even though runoffs are projected to be higher than baseline period. According to the study carried out by Wilson and Weng (2011), climate change potential to alter suspended sediment concentration levels was higher than the potential of land use change.

The results of combined impacts of climate and land use change on total ammonia and orthophosphate are indicated in Fig. 8c, d. The changes in total ammonia generally followed the pattern of climate change scenarios. Concentrations were decreased all months with a maximum decrease of 41% under HCC-LC30 and a minimum decrease of 1.7% under LCC-LC60 (Fig. 8c). Maximum changes in total ammonia concentrations were associated with HCC-LC30 scenario due to the direction of changes in urban development scenario. As shown in Fig. 7c, urban development (LC30) presented no change in total ammonia concentration compared to agricultural development (LC60) which showed increases in concentrations. This opposite direction of changes caused by LC60 was the reason for the maximum decrease in concentrations associated with HCC-LC30. This scenario was valid for changes in orthophosphate concentrations. As indicated in Fig. 8d, HCC-LC30 was the dominant scenario of a decrease in concentrations. Orthophosphate concentrations were increased in late winter and early spring months (January through March) under two combined scenario of HCC-LC60 and LCC-LC60. This can be explained by an increase in suspended sediment and orthophosphate concentrations under agricultural land development scenario (LC60). This result indicates the importance of land use change on nutrient changes and strong relationship between suspended sediment and orthophosphate as confirmed by previous studies (Tu 2009; Hadjikakou et al. 2011; Praskievicz and Chang 2011; Wilson and Weng 2011; Tong et al. 2012; El-Khoury et al. 2015).

It should be noted that in this study we only used one climate change model (CCSM4.0) and two climate change scenarios (RCP 2.6 and RCP 8.5). Using more climate change models and scenarios will provide more clear and profound results on how climate and land use change impact water quantity and quality in the Kor River watershed. Furthermore, land use change scenarios were developed in this study based on the historical rate of land use change, assuming that future rates affected by the current rate of land use changes. Further research might require in

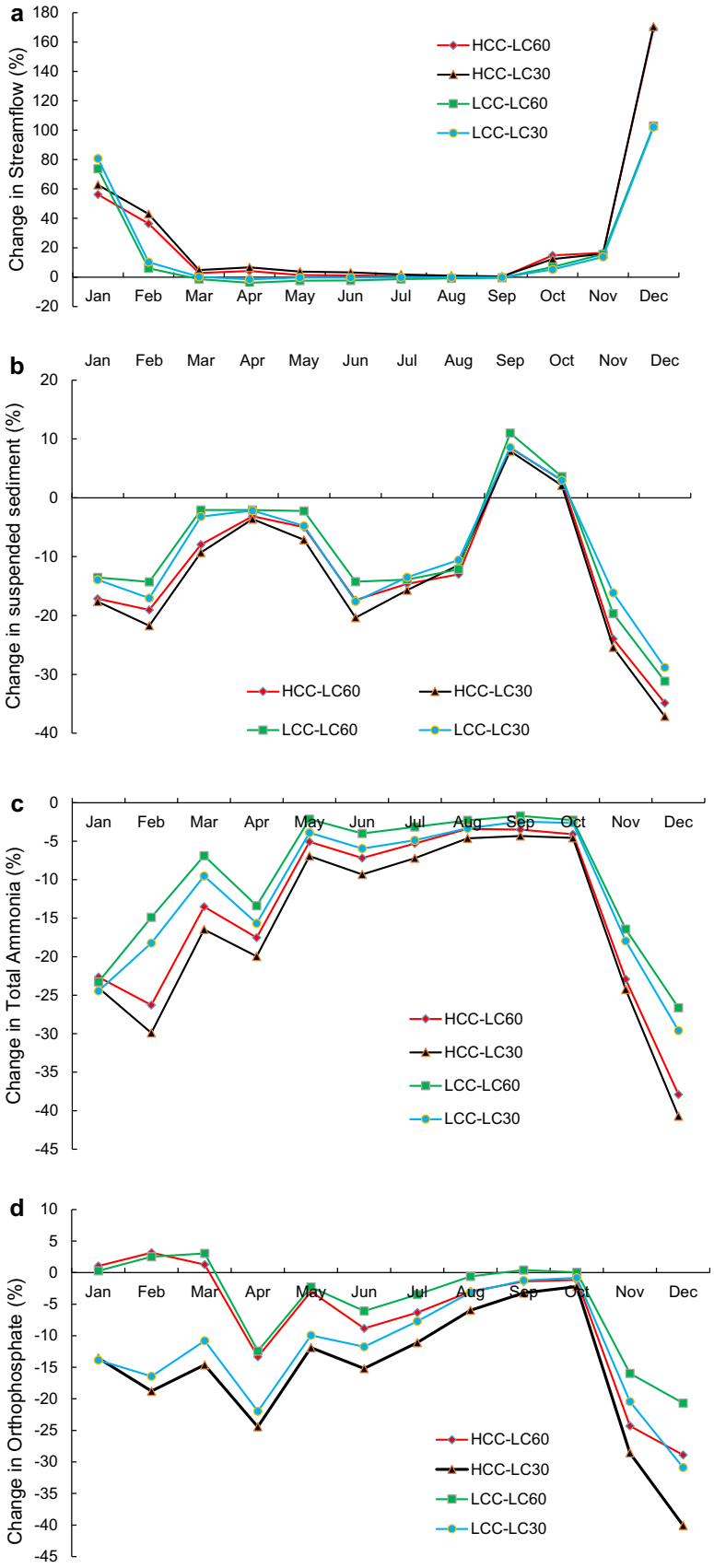

Fig. 8 Change in **a** streamflow, **b** suspended sediment, **c** total ammonia, **d** orthophosphate concentration in the future period (2020–2049) relative to the baseline simulations (2003–2012) under combined change scenarios

order to address more precise land use changes in the future. However, besides the limitations and assumptions, the results of this study provide relevant and useful information for investigating the combined impacts of climate and land use change on water quantity and quality.

Conclusions

This research addressed the separate and combined impacts of climate and land use change on streamflow, suspended sediment, total ammonia and orthophosphate concentrations. BASINS–WinHSPF model is used in order to simulate future changes under different climate and land use change scenarios. The model calibrated and validated for hydrology, sediment and water quality for the period 2003–2012. The good agreement between observed and simulated daily values confirmed that calibrated WinHSPF could be applied to evaluate the responses of Kor River Basin to climate and land use changes. One climate change model (CCSM4.0) and two climate change scenarios RCP 2.6 and RCP 8.5 based on IPCC Fifth Assessment Report (AR5) along with two future land use change scenarios (Agricultural development LC60 and Urban development LC30) established. Predicted changes were for near-future period 2020–2049. Combined scenarios were setup-based climate and land use change scenarios.

The results revealed that projected climate change impacts include an increase in streamflow and mostly decrease in suspended sediment, total ammonia and orthophosphate concentrations. For land use change scenarios, agricultural development scenario (LC60) indicated an opposite direction of changes in total ammonia and orthophosphate, leading to the conclusion that land use change is the dominant factor in nutrient concentration changes. Combined impacts results indicated that general pattern of changes in streamflow, suspended sediment and water quality parameters tracked the results of climate change scenarios. Additionally, according to combined impacts, land use change scenarios had important impacts on the direction of changes in nutrient concentrations.

The results presented here are subject to uncertainties inherent in any scenario-based analysis. Uncertainties associated with climate model output, downscaling method and the hydrological model are not included in our study. We will aim to address these uncertainties in our future researches. By considering limitations of this study, it can be concluded that examining separate and combined impacts of climate and land use change is useful for water resource managers and decision makers in order to prepare and adapt strategies to mitigate negative impacts of climate and land use changes in the watershed.

References

Abbaspour KC, Faramarzi M, Ghasemi SS, Yang H (2009) Assessing the impact of climate change on water resources in Iran. Water Resour Res 45:1–16. doi:10.1029/2008WR007615

Albek M, Albek E (2003) Predicting the effects of climate change on the sediment yield of watersheds. In: Diffuse pollution conference dublin 2003 3G: Agriculture, pp 137–142

Astaraie-Imani M, Kapelan Z, Fu G, Butler D (2012) Assessing the combined effects of urbanisation and climate change on the river water quality in an integrated urban wastewater system in the UK. J Environ Manag 112:1–9. doi:10.1016/j.jenvman.2012.06.039

Bicknell BR, Imhoff JC, Kittle Jr JL, Jobes TH, Donigian Jr AS (2001) Hydrological simulation program—FORTRAN (HSPF) Version 12, User's Manual, 2001

Cox BA, Whitehead PG (2009) Impacts of climate change scenarios on dissolved oxygen in the River Thames, UK. Hydrol Res 40:138. doi:10.2166/nh.2009.096

Crossman J, Futter MN, Oni SK, Whitehead PG, Jin L, Butterfield D, Baulch HM, Dillon PJ (2013) Impacts of climate change on hydrology and water quality: future proofing management strategies in the Lake Simcoe watershed, Canada. J Great Lakes Res 39:19–32. doi:10.1016/j.jglr.2012.11.003

Dixon B, Earls J (2012) Effects of urbanization on streamflow using SWAT with real and simulated meteorological data. Appl Geogr 35:174–190. doi:10.1016/j.apgeog.2012.06.010

Duda PB, Hummel PR, Donigian ASJ, Imhoff JC (2012) Basins/Hspf: model use, calibration, and validation. Trans Asabe 55:1523–1547. doi:10.13031/2013.42261

El-Khoury A, Seidou O, Lapen DRL, Que Z, Mohammadian M, Sunohara M, Bahram D (2015) Combined impacts of future climate and land use changes on discharge, nitrogen and phosphorus loads for a Canadian river basin. J Environ Manag 151:76–86. doi:10.1016/j.jenvman.2014.12.012

Etemadi H, Samadi SZ, Sharifikia M (2012) Stastistical downscaling of climate variables in Shadegan Wetland, Iran. Sci Rep 1:1–9. doi:10.4172/scientificrep

Fakhraei H (2009) Determination of self assimilating capacity of Kor and Sivand Rivers and total maximum daily load allocation (TMDL) of their pollution sources. Shiraz University, Shiraz

Fan M, Shibata H (2015) Simulation of watershed hydrology and stream water quality under land use and climate change scenarios in Teshio River watershed, northern Japan. Ecol Indic 50:79–89. doi:10.1016/j.ecolind.2014.11.003

Fernandes MR, Segurado P, Jauch E, Ferreira MT (2016) Riparian responses to extreme climate and land-use change scenarios. Sci Total Environ 569–570:145–158. doi:10.1016/j.scitotenv.2016.06.099

Ficklin DL, Stewart IT, Maurer EP (2013) Effects of climate change on stream temperature, dissolved oxygen, and sediment concentration in the Sierra Nevada in California. Water Resour Res 49:2765–2782. doi:10.1002/wrcr.20248

Hadjikakou M, Whitehead PG, Jin L, Futter M, Hadjinicolaou P, Shahgedanova M (2011) Modelling nitrogen in the Yeilirmak River catchment in Northern Turkey: impacts of future climate and environmental change and implications for nutrient management. Sci Total Environ 409:2404–2418

Hamon RW (1961) Estimating potential evapotranspiration. J Hydraul Div 87(HY3):107–120

Jin L, Whitehead PG, Futter MN, Lu Z (2012) Modelling the impacts of climate change on flow and nitrate in the River Thames: assessing potential adaptation strategies. Hydrol Res 43:902–916. doi:10.2166/nh.2011.080

Jones PD, Hulme M (1996) Calculating regional climatic time series for temperature and precipitation: methods and illustrations. Int J Climatol 16:361–377. doi:10.1002/(SICI)1097-0088(199604)16:4<361:AID-JOC53>3.0.CO;2-F

Kim SM, Benham BL, Brannan KM, Zeckoski RW, Doherty J (2007) Comparison of hydrologic calibration of HSPF using automatic and manual methods. Water Resour Res. doi:10.1029/2006WR004883

Kim J, Choi J, Choi C, Park S (2013) Impacts of changes in climate and land use/land cover under IPCC RCP scenarios on streamflow in the Hoeya River Basin, Korea. Sci Total Environ 452–453:181–195. doi:10.1016/j.scitotenv.2013.02.005

Li Z, Huang G, Wang X, Han J, Fan Y (2016) Impacts of future climate change on river discharge based on hydrological inference: a case study of the Grand River Watershed in Ontario, Canada. Sci Total Environ 548–549:198–210. doi:10.1016/j.scitotenv.2016.01.002

Mehdi B, Ludwig R, Lehner B (2015) Evaluating the impacts of climate change and crop land use change on streamflow, nitrates and phosphorus: a modeling study in Bavaria. J Hydrol Reg Stud 4:60–90. doi:10.1016/j.ejrh.2015.04.009

Mitsova D (2014) Coupling land use change modeling with climate projections to estimate seasonal variability in runoff from an urbanizing catchment near Cincinnati, Ohio. ISPRS Int J Geo Inf 3:1256–1277. doi:10.3390/ijgi3041256

Mohsenipour M, Shahid S, Nazemosadat MJ (2013) Effects of El Nino-Southern oscillation on the discharge of Kor River in Iran. Adv Meteorol 2013:1–4. doi:10.1155/2013/846397

Mukundan R, Pradhanang SM, Schneiderman EM, Pierson DC, Anandhi A, Zion MS, Matonse AH, Lounsbury DG, Steenhuis TS (2013) Suspended sediment source areas and future climate impact on soil erosion and sediment yield in a New York City water supply watershed, USA. Geomorphology 183:110–119. doi:10.1016/j.geomorph.2012.06.021

Nash JE, Sutcliffe JV (1970) River flow forecasting through conceptual models part I—a discussion of principles. J Hydrol 10:282–290. doi:10.1016/0022-1694(70)90255-6

Pervez MS, Henebry GM (2015) Assessing the impacts of climate and land use and land cover change on the freshwater availability in the Brahmaputra River basin. J Hydrol Reg Stud 3:285–311. doi:10.1016/j.ejrh.2014.09.003

Praskievicz S (2016) Impacts of projected climate changes on streamflow and sediment transport for three snowmelt-dominated rivers in the interior Pacific Northwest. River Res Appl 32:4–17. doi:10.1002/rra.2841

Praskievicz S, Chang H (2009) A review of hydrological modelling of basin-scale climate change and urban development impacts. Prog Phys Geogr 33:650–671. doi:10.1177/0309133309348098

Praskievicz S, Chang H (2011) Impacts of climate change and urban development on water resources in the Tualatin River Basin, Oregon. Ann Assoc Am Geogr 101:249–271. doi:10.1080/00045608.2010.544934

Rehana S, Mujumdar PP (2011) River water quality response under hypothetical climate change scenarios in Tunga–Bhadra river, India. Hydrol Process 25:3373–3386. doi:10.1002/hyp.8057

Rodriguez-Lloveras X, Buytaert W, Benito G (2016) Land use can offset climate change induced increases in erosion in Mediterranean watersheds. CATENA 143:244–255. doi:10.1016/j.catena.2016.04.012

Ruiter A (2012) Delta-change approach for CMIP5 GCMs. Utrecht

Shrestha B, Babel MS, Maskey S, Van Griensven A, Uhlenbrook S, Green A, Akkharath I (2013) Impact of climate change on sediment yield in the Mekong River basin: a case study of the Nam Ou basin, Lao PDR. Hydrol Earth Syst Sci 17:1–20. doi:10.5194/hess-17-1-2013

Taylor KE, Stouffer RJ, Meehl GA (2012) An overview of CMIP5 and the experiment design. Bull Am Meteorol Soc 93:485–498. doi:10.1175/BAMS-D-11-00094.1

Thodsen H, Hasholt B, Kjærsgaard JH (2008) The influence of climate change on suspended sediment transport in Danish rivers. Hydrol Process 22:764–774. doi:10.1002/hyp.6652

Tong STY, Sun Y, Ranatunga T, He J, Yang YJ (2012) Predicting plausible impacts of sets of climate and land use change scenarios on water resources. Appl Geogr 32:477–489. doi:10.1016/j.apgeog.2011.06.014

Tu J (2009) Combined impact of climate and land use changes on streamflow and water quality in eastern Massachusetts, USA. J Hydrol 379:268–283. doi:10.1016/j.jhydrol.2009.10.009

Tu J, Xia Z (2008) Examining spatially varying relationships between land use and water quality using geographically weighted regression I: model design and evaluation. Sci Total Environ 407(1):358–378. doi:10.1016/j.scitotenv.2008.09.031

Ward PJ, van Balen RT, Verstraeten G, Renssen H, Vandenberghe J (2009) The impact of land use and climate change on late Holocene and future suspended sediment yield of the Meuse catchment. Geomorphology 103:389–400. doi:10.1016/j.geomorph.2008.07.006

Whitehead PG, Johnes PJ, Butterfield D (2002) Steady state and dynamic modelling of nitrogen in the River Kennet: impacts of land use change since the 1930s. Sci Total Environ 282–283:417–434. doi:10.1016/S0048-9697(01)00927-5

Whitehead PG, Wilby RL, Butterfield D, Wade AJ (2006) Impacts of climate change on in-stream nitrogen in a lowland chalk stream: an appraisal of adaptation strategies. Sci Total Environ 365:260–273. doi:10.1016/j.scitotenv.2006.02.040

Whitehead PG, Sarkar S, Jin L, Futter MN, Caesar J, Barbour E, Butterfield D, Sinha R, Nicholls R, Hutton C, Leckie HD (2015) Dynamic modeling of the Ganga river system: impacts of future climate and socio-economic change on flows and nitrogen fluxes in India and Bangladesh. Environ Sci Impacts 17:1082–1097. doi:10.1039/c4em00616j

Wilson CO, Weng Q (2011) Simulating the impacts of future land use and climate changes on surface water quality in the Des Plaines River watershed, Chicago Metropolitan Statistical Area, Illinois. Sci Total Environ 409:4387–4405. doi:10.1016/j.scitotenv.2011.07.001